Scientific Research Publishing

Journal of Computer and Communications, 2022, 10, 171-196
https://www.scirp.org/journal/jcc
ISSN Online: 2327-5227
ISSN Print: 2327-5219

Propagation Model Optimization Based on Ion Motion Optimization Algorithm for Efficient Deployment of eLTE Network

Deussom Djomadji Eric Michel[1,2,3], Tsague Njatsa Austene Beldine[2], Tonye Emmanuel[3]

[1]Department of Electrical and Electronic Engineering, College of Technology, University of Buea, Buea, Cameroon
[2]Division of Information and Communications Technology, NASPT, University of Yaoundé I, Yaoundé, Cameroon
[3]Department of Electrical and Telecommunications, University of Yaoundé I, Yaoundé, Cameroon
Email: eric.deussom@gmail.com

How to cite this paper: Michel, D.D.E., Beldine, T.N.A. and Emmanuel, T. (2022) Propagation Model Optimization Based on Ion Motion Optimization Algorithm for Efficient Deployment of eLTE Network. *Journal of Computer and Communications*, **10**, 171-196.
https://doi.org/10.4236/jcc.2022.1011012

Received: October 18, 2022
Accepted: November 27, 2022
Published: November 30, 2022

Abstract

Propagation models are the foundation for radio planning in mobile networks. They are widely used during feasibility studies and initial network deployment, or during network extensions, particularly in new cities. They can be used to calculate the power of the signal received by a mobile terminal, evaluate the coverage radius, and calculate the number of cells required to cover a given area. This paper takes into account the standard K factors model and then uses the Ion motion optimization (IMO) algorithm to set up a propagation model adapted to the physical environment of each of the Cameroonian cities of Yaoundé and Bertoua for different frequencies and technologies. Drive tests were made on the CDMA network in the city of Yaoundé on one hand and on an LTE TDD network in the city of Bertoua on the other hand. IMO is used as the optimization algorithm to deduct a propagation model which fits the environment of the two considered towns. The calculation of the root-mean-square error (RMSE) between the actual data from the drive tests and the prediction data from the implemented model allows the validation of the obtained results. A comparative study made between the RMSE value obtained by the new model and those obtained by the Okumura-Hata and K factors standard models, allowed us to conclude that the new model obtained in each of these two cities is better and more representative of our local environment than the Okumura-Hata currently implemented. The implementation shows that IMO can perform well and solve this kind of optimization problem; the newly obtained models can be used for radio planning in the cities of Yaounde and Bertoua in Cameroon.

Keywords

Drive Test, IMO, Propagation Models, Root Mean Square Error

1. Introduction

Many researchers have worked and proposed numerous algorithms with inspiration from nature for solving various optimization problems. Some of the most popular are Genetic Algorithm (GA) [1] [2] [3] [4] [5], Particle Swarm Optimization (PSO) [6] [7] [8] [9], and Artificial Bee Colony (ABC) [10] [11] [12] [13] [14]. These algorithms have advantages and disadvantages compared to each other and may show different performances when solving discrete and continuous problems.

A new physics-inspired metaheuristic optimization algorithm based on the motion of ions in nature called Ion Motion Optimization (IMO) was published in 2015 [15]. It is gradually being used to solve problems in various fields, particularly in the field of transport [16]; in the field of computing for solving the problem of optimizing node coverage in wireless sensor networks [17], in the field of chemistry [18], and many other fields. As IMO is a newly developed algorithm through this work we also test and evaluate its capability to solve this kind of optimization problem, the one of building an appropriated propagation model related to any kind of environment.

The objective of this study is to integrate the use of the IMO algorithm in the resolution of a real problem in the field of telecommunications, which is optimizing propagation models. Based on the hypothesis that the standard propagation models currently implemented in Cameroon have been developed in other countries and therefore do not accurately reflect the characteristics of the physical environment of Cameroonian cities; IMO, a new population-based algorithm whose performance has been evaluated through ten standard test functions as well as three real problems and whose results provided are very competitive with well-known algorithms in the same field [16], would be appropriate to optimize the Okumura-Hata propagation model. In our study; we will in the first part evaluate and validate the performance of the IMO algorithm in solving complex problems through drive test data collected in the existing CDMA 1X EVDO REVB network in 800 MHz band of Yaoundé and we will apply it in the optimization of the Okumura-Hata propagation model in the LTE TDD network in 380 - 400 MHZ band of the city of Bertoua. We know that CDMA 1X EVDO REVB technology is disappearing, however the 800 MHz frequency band is a so-called golden frequency, due to its use in new generations of mobile telephony and the wave propagation is not technology bind.

This work is not the first to focus on the optimization of propagation models. Indeed, several people from various backgrounds have already addressed the issue, each tackling a specific aspect of the problem or part of the network. For example, Deussom Eric and Tonye Emmanuel [19] worked on "New Propagation Model Optimization Approach based on Particles Swarm Optimization Algorithm"; Deussom Eric and Tonye Emmanuel [20] worked on "Propagation model optimization based on Artificial Bee Colony algorithm: Application to Yaoundé town, Cameroon; Deussom eric *et al.* has used Social Spider Algorithm

in [21] for Propagation Model Optimization. Deussom Eric and Tonye Emmanuel have also proposed other methods for propagation model optimization in [22] [23] [24] [25]

This article will be articulated as follow: in Section 2; the experimental details will be presented; followed by a description of the methodology adopted in Section 3. The results of the implementation of the algorithm; the validation of the results and comments will be provided in Section 4 and finally a conclusion will be presented in Section 5.

2. Experimental Details

2.1. Propagation Environment

The city of Yaoundé, capital of Cameroon is the one on which the present study is based at first. We relied on the existing CDMA 2000 1X_EVDO network to make radio measurements. To do this, 3 categories of areas were chosen in the city of Yaoundé namely: Dense urban area (Center town, Bastos), the urban area (Biyem-Assi, camp Sonel Essos), the suburban area (Awae district and Ngousso-Eleveur district) corresponding respectively to areas with high, medium and low population agglomerations. Table 1 shows the areas chosen with the BTS concerned.

Following the same principle, for the case of Bertoua City (regional capital of east region with a different type of urbanization compare to Yaoundé town), we selected 3 areas namely Bertoua Lycee, Bertoua central and Bertoua CRTV.

2.2. Equipment Description

2.2.1. Simplified Description of BTS Used

BTS that we used for our drive tests are the ones of the telephony operator CAMTEL provided by the equipment manufacturer HUAWEI Technologies. 2 types of BTS have been taken into account namely BTS3606 and DBS3900 all CDMA. Table 2 shows the technical specifications of these BTS.

The radio parameters of the BTS of the city center, Bastos, Biyem-Assi, Essos, Awae and Ngousso are presented in Table 3.

2.2.2. Simplified Description of eNodeB Used

For the Case of Bertoua the enodeB used for drive tests is provided by Huawei, DBS3900 LTE TDD working in the frequency band of 380 - 400 MHz. Table 4 presents the radio parameters used on this eLTE network.

Table 1. Types of environment.

Categories	A	B	C
Urban feature	Dense urban (Center town, Bastos)	Urban (Biyem-Assi, Essos)	suburban (Awae, Ngousso)
BTS concerned	Ministry PTT (A1) Camtel Bastos (A2)	Biyem-Assi (B1) Hotel du plateau (B2)	Nkomo-Awae (C1) Ngousso-eleveur (C2)

Table 2. BTS characteristics.

Nature	BTS3606	DBS3900
Type of BTS	Compact Indoor	Outdoor Distributed
Number of sectors	3	3
Frequency band	Band Class 0 (800 Mhz)	Band Class 0 (800 Mhz)
Downward frequency	869 MHz to 894 MHz	869 MHz to 894 MHz
Rising frequency	824 MHz to 849 MHz	824 MHz to 849 MHz
Max power (single carrier)	20 W	20 W
Total power of the BTS (dBm)	43 dBm	43 dBm

Table 3. BTS engineering parameters.

BTS Informations									
Type BTS	**BTS Name**	**Latitude**	**Longitude**	**BTS Altitude (m)**	**Antenna height**	**Average elevation**	**Effective antenna Height**	**Anten na gain (dBi)**	**7/8 Feeder Cable (meter)**
3606	Ministry PT_800	3.86587	11.5125	749	40	741.82	47.18	15.5	45
3900	Nkomo Awae	3.83224	11.5598	713	25	709.54	28.46	17	0
3606	Biyem-Assi_800	3.83441	11.4854	721	40	709.54	51.46	15.5	45
3900	Ngousso-eleveur	3.90097	11.5613	716	25	712.05	28.95	17	0
3900	Hotel du plateau	3.87946	11.5503	773	27	753.96	46.04	17	0
3900	Camtel Bastos	3.89719	11.50854	770	28	754.86	43.14	17	0

Table 4. Radio parameters.

ENODEB RADIO PARAMETERS: Frequency 380 MHz				
Sector ID	**PCI**	**Azimuth**	**Antenna Height**	**Tilt**
		Bertoua CRTV		
0	189	25	30	3
1	191	143	30	6
2	190	240	30	0
		Bertoua Central		
0	185	344	25	6
1	183	120	25	3
2	184	240	25	3
		Bertoua Lycée		
0	188	300	20	6
1	186	80	20	2
2	187	195	20	6

2.2.3. Other Equipment Parameters

To perform the drive tests. We used a Toyota Prado VX vehicle, an ACER ASPIRE laptop, drive test software namely Pilot pioneer of Dingli communication V6.0, an LG CDMA mobile terminal, a GPS terminal, a DC/AC converter to

power the PC during the measurement. The town of Yaoundé has been selected because it is the capital of Cameroun. While Bertoua town is the regional capital of east region, Bertoua doesn't have the same development like Yaoundé, and the urbanization of the 02 town are different, then we have selected them to have a kind of diversity, a big town and a middle one.

The drive test done in Yaoundé, the capital of Cameroon gave the following results:

Dense Urban Area

The following Figures 1-3 present some drive tests results in some of the areas of the town of Yaoundé.

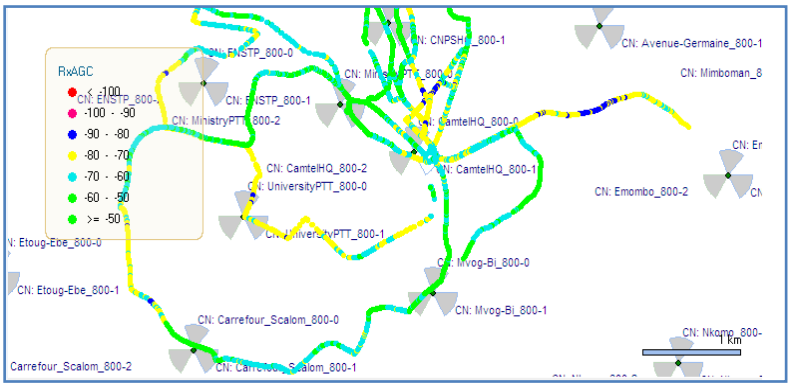

Figure 1. drive test in center town.

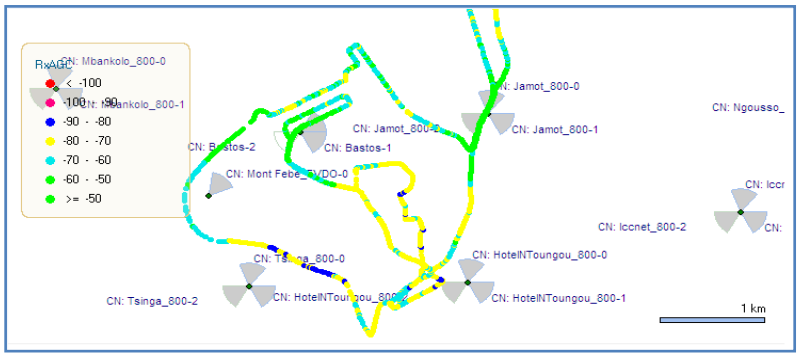

Figure 2. Drive test in Bastos.

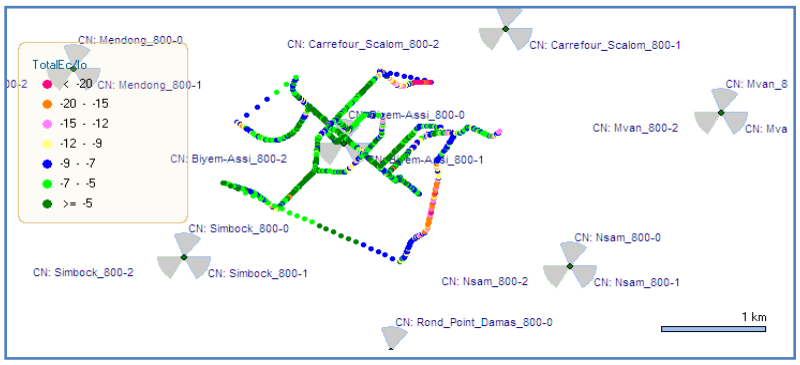

Figure 3. Drive test in Biyem-Assi.

For the case of Bertoua town, which is a regional capital for east region in Cameroon, and where the urban environment is different to the one of Yaoundé, we have the drive tests done in 3 areas presented in the following Figures 4-6:

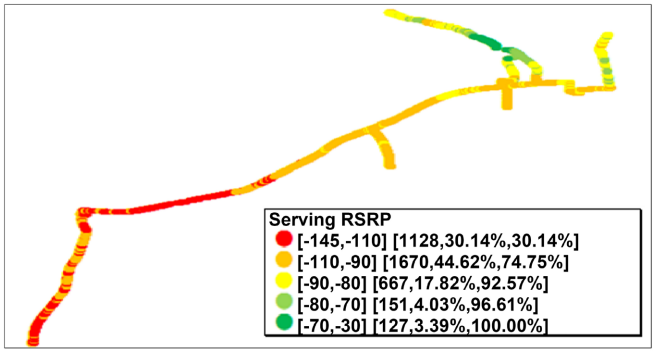

Figure 4. Drive Test Result of Bertoua CRTV.

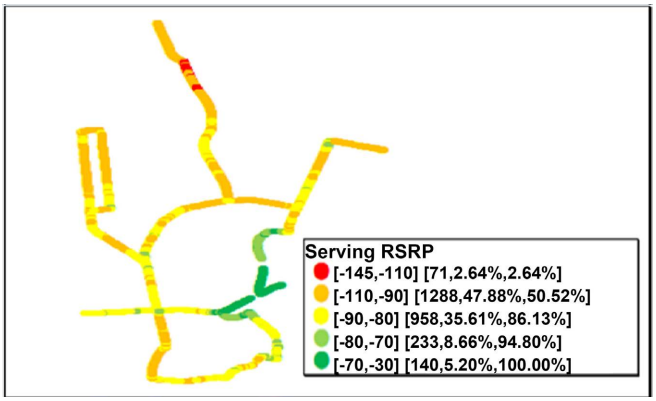

Figure 5. Drive test result of Bertoua Central.

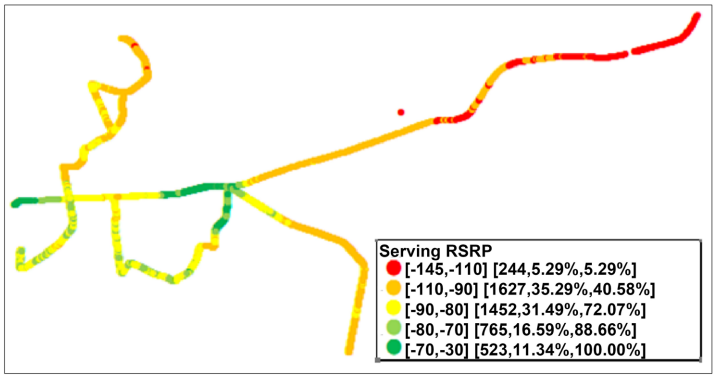

Figure 6. Drive test result of Bertoua Lycée.

3. Methodology

3.1. Propagation Model

Many propagation models exist in scientific literature, we present only the Okumura-Hata, free space and K factors models on which we relied for this work. The distance d is expressed in km and the frequency f in MHz.

3.1.1. Propagation Model *K* Factors

1) Description

The general shape of the K factor model [16] is given by the relation below:

$$L = K_1 + K_2 \times \log(d) + K_3 \times h_m + K_4 \times \log(h_m) + K_5 \times \log(h_b) + K_6 \times \log(h_b)\log(d) + K_{7\text{diff}} + K_{\text{clutter}} \quad (1)$$

The values of the K parameters vary according to the type of terrain and the characteristics of the propagation environment of the h_m, h_b; Valid heights of the BS antenna and the MS antenna in meters.

d is the distance between the base station and the mobile station (km); Table 5 shows values of K and the attenuation factor due to congestion for a medium-sized city.

The previous equation can be rewritten as follows:

$$L = (K_1 + K_{7\text{diff}} + K_{\text{clutter}}) + K_2 \times \log(d) + K_3 \times h_m + K_4 \times \log(h_m) + K_5 \times \log(h_b) + K_6 \times \log(h_b)\log(d) \quad (2)$$

By taking, $K_1' = (K_1 + K_{7\text{diff}} + K_{\text{clutter}})$, the equation of the model K factor becomes:

$$L = K_1 + K_2 \times \log(d) + K_3 \times h_m + K_4 \times \log(h_m) + K_5 \times \log(h_b) + K_6 \times \log(h_b)\log(d) \quad (3)$$

The previous Equation (3) can be written into two forms, a factorized form as a function of a column vector that will be specified in the sequence and a linear form but in the context of our study, we consider only the factorized form.

2) Factorized Form of the Propagation Model *K* Factors

The factorized form of the model K factors is written

$$L = [K_1 K_2 K_3 K_4 K_5 K_6] \times \begin{bmatrix} 1 \\ \log(d) \\ h_m \\ \log(h_m) \\ \log(h_b) \\ \log(h_b)\log(d) \end{bmatrix} \quad (4)$$

In the previous equation letting $K = [K_1 K_2 K_3 K_4 K_5 K_6]$ and

$$M = \begin{bmatrix} 1 \\ \log(d) \\ h_m \\ \log(h_m) \\ \log(h_b) \\ \log(h_b)\log(d) \end{bmatrix} \quad (5)$$

Table 5. K values of model K factors for a medium city [16].

K parameters	K_1	K_2	K_3	K_4	K_5	K_6	$K_{7\text{diff}}$	K_{clutter}
Parameter value	149	44.9	−2.49	0.00	−13.82	−6.55	−0.8	0

It follows that, the propagation model K factors can be written as

$$L = K \times M \ . \tag{6}$$

This expression will be considered as the factorized form of the propagation model.

3.1.2. Okumura Hata and Free Space Models [16]

The Okumura-Hata and free space models are special cases of the K factor models.

The expression of the Okumura-Hata model is written as follows:

$$L = 69.55 + 26.16\log(f_c) - 13.82\log(h_b) + \left(44.9 - 13.82\log(h_b)\right)\log(r) - E \tag{7}$$

with

$$= 3.2\left(\log(11.75h_m)\right)^2 - 4.497 \ . \tag{8}$$

h_b is the height of the base station. r the coverage radius of a site. $h_m = 1.5$ m represents User's quipment antenna the height. For this value of h_m, $E = -9.2 \times 10^{-4}$ which is negligible.

Subsequently, E will therefore be assimilated to the value $E = 0$.

The free space model is expressed by the relation:

$$L = 32.45 + 20\log(f_c) + 20\log(r) \tag{9}$$

The K values for these two models are as follows in Table 6.

3.2. Propagation Model Optimization Using IMO

3.2.1. Inspiration

The word "ion" is a Greek term. The English physician Michael Faraday introduced this term in 1834. In general, charged particles are called ions and can be divided into two types:

Anions: negatively charged ions (−);

Cations: positively charged ions (+).

The main inspiration for the IMO algorithm is the fact that ions with similar charges tend to repel each other, while ions with opposite charges tend to attract to each other (Figure 7).

The attraction and repulsion forces between anions and cations are also depicted in Figure 8. The candidate solutions for a given optimization problem in the IMO algorithm are divided into two groups anions (negative ions) and cations (positive ions). The ions represent candidate solutions for a particular problem and attraction/repulsion forces move the ions around the search space. We require the IMO algorithm's ions to move toward the best ions with opposite

Table 6. K values for the Okumura-Hata model and free space.

Model	K_1	K_2	K_3	K_4	K_5	K_6
Okumura hata	$69.55 + 26.16\log(f_c) - E$	44.9	0	0	13.82	−6.55
Free Space	$32.45 + 20\log(f_c)$	20	0	0	0	0

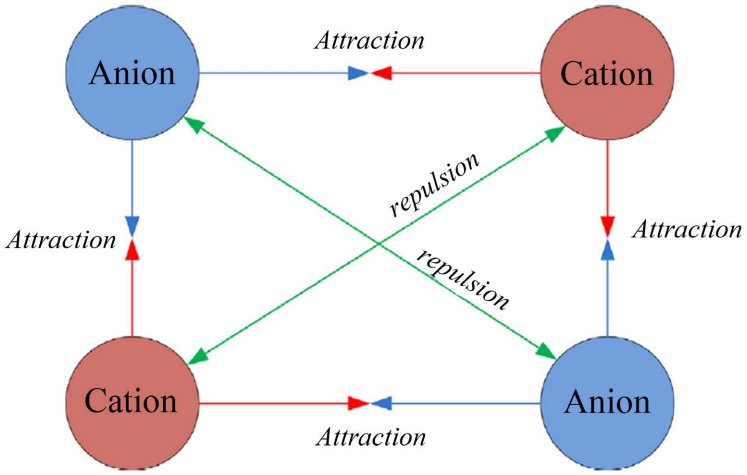

Figure 7. Conceptual model and forces of attraction and repulsion of anions and cations [16].

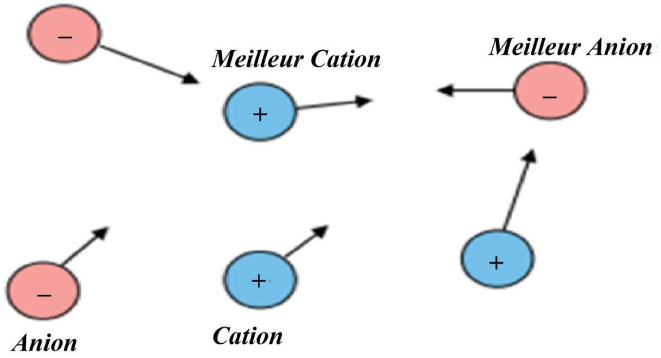

Figure 8. Movement of ions to the best ions in the liquid phase [16].

charges. The ions are evaluated based on their fitness, so the fitness of ions is proportional to the value of the objective function. Needless to say, anions move toward the best cation, whereas cations move toward the best anion. Their amount of movement depends on the attraction/repulsion forces between them. The magnitude of this force specifies the momentum of each ion. So far, the movement of ions in the IMO algorithm can guarantee the improvement of all ions throughout iterations. However, there are no mechanisms for diversification and intensification. To require the ions to diversify and intensify, we assume that the ions can be in two completely different phases: liquid versus solid.

3.2.2. IMO Algorithm Execution Phases

In the IMO algorithm, the movement of ions is carried out in two main phases, in particular the liquid phase representing the diversification and the crystalline phase representing the intensification.

1) Liquid phase (Diversification)

In the liquid phase the ions have greater freedom of movement. In addition, the forces of attraction between ions of opposite charges are greater than the forces of repulsion between ions of similar charges. This is why in the IMO algo-

rithm the forces of repulsion are ignored in this phase to explore the search space. The mathematical model is presented as follows:

- **Calculation of the forces of attraction between the ions**

The calculation of the forces of attraction is a function of the distance that separates the ions and the best ions from opposite charges.

$$AF_{i,j} = \frac{1}{1+e^{-0.1/AD_{i,j}}} \tag{10}$$

$$CF_{i,j} = \frac{1}{1+e^{-0.1/CD_{i,j}}} \tag{11}$$

with

$$AD_{i,j} = \left| A_{i,j} - Cbest_j \right| \tag{12}$$

and

$$CD_{i,j} = \left| D_{i,j} - Abest_j \right| \tag{13}$$

i indicates the index of the ion and j the dimension.

$AD_{i,j}$ represents the distance between the ith anion and the best cation in dimension j; $CD_{i,j}$ represents the distance between the ith cation and the best anion in dimension j. $AF_{i,j}$ is the resultant force of attraction of the anions and $CF_{i,j}$ the resulting force of attraction of the cations.

According to Equations (10) and (11) above, the forces between ions are inversely proportional to the distances between them. The greater the distance, the lower the force of attraction. In other words, when the distance of the ions from the best ion of opposite charge becomes greater, a weaker force of attraction is applied to them.

According to these same equations, the force of attraction varies between 0.5 and 1 [16].

- **Updating the positions of Anions and Cations**

After the attraction force calculation, the position of the anions and cations is updated as follows:

$$A_{i,j} = A_{i,j} + AF_{i,j} \times \left(Cbest_j - A_{i,j} \right) \tag{14}$$

$$C_{i,j} = C_{i,j} + CF_{i,j} \times \left(Abest_j - C_{i,j} \right) \tag{15}$$

According to these two previous equations, only the force element determines the movement of each ion to the best ion of opposite charge. $Cbest_j$ and $Abest_j$ indicate the best cation and the best anion respectively.

We can deduce from previous mathematical models that there is no random component involved in the liquid phase. However, since the movements are proportional to the distances, the ions diversify around the search space. As ions tend to be attracted to other ions with opposite charges, exploration/diversification can be guaranteed. With the increase in the number of iterations, more ions interact and converge to the best ions with opposite charges and diversification is gradually reduced. The displacement of ions to the best opposite charge ions in

the liquid phase is as follows:

The search agents of the IMO algorithm also enter the crystalline phase which means that they eventually converge on a solution in the search space. The crystalline phase is presented below.

2) Crystalline phase (Intensification)

In the Crystalline Phase, the ions have converged at an optimal point and convergence occurred. However, due to the unknown shape of the research space, it could be that the convergence in question took place at a local optimum. Therefore, a mechanism is implemented for ions in the crystalline phase to excite the trapped ions out of the local optimum. The mechanism implemented in the crystalline phase is illustrated by the following diagram (**Figure 9**).

The algorithm representing the mathematical modeling of this phenomenon to solve the local trapping of the optimum is as follows:

Begin

If $(CbestFit >= \frac{\text{CworstFit}}{2}$ and $\text{AbestFit} >= \frac{\text{AworstFit}}{2})$

if rand ( ) > 0.5

$A_i = A_i + Q1 \times (Cbest - 1)$

else

$A_i = A_i + Q1 \times (Cbest)$

End if

if rand () > 0.5

$C_i = C_i + Q2 \times (Abest - 1)$

else

$C_i = C_i + Q2 \times (Abest)$

End if

if rand () < 0.05

Reset A_i and C_i

End if

End if

End (16)

Q_1 and Q_2 are random numbers within the range [−1, 1] and rand ( ) is a function that returns a random number within the interval [0, 1].

According to the pseudo-code here is a condition for moving from the liquid state to the solid state the average ability of the worst ions must be less than or equal to the ability of the best ions. If this condition is met, the anions and cations are randomly distributed around the best cation and anion respectively.

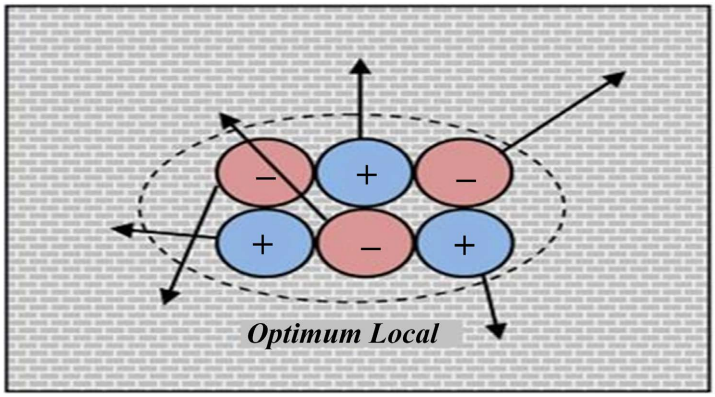

Figure 9. Motion of ions around an optimum in the crystal phase [16].

CworstFit and CbestFit are respectively the ability of the worst and the best cation. In addition, AworstFit and AbestFit are the ability of the worst and the best anion. To increase diversity, several anions and cations are eventually reset with low probability.

In order to better understand the behavior of the proposed IMO algorithm, some comments on the novel concepts and ideas as well as their effects on the performance of the proposed algorithms are as follows:

- The proposed method of interaction between the search agents (ions) of the IMO algorithm using attraction and repulsion forces are novel [15], which assist the search agent to move around the search space and explore diverse regions of search spaces.
- The proposed equations for simulating liquid phase cause convergence of search agents toward the recent best solutions found so far. This approach guarantees the convergence of the IMO algorithm toward the best solutions during optimization [15].
- The proposed equations and conditions for simulating the crystal phase are useful for resolving local optima stagnation. The liquid phase may cause the search agents to be trapped in local solutions quickly. However, the crystal phase resolves such cases by relocating the search agents around the search space suddenly and stochastically.

3.2.3. IMO Algorithm Execution Flowchart

The different phases of the IMO algorithm have been clearly explained above, we present here the organization chart of the sequence of these different phases (**Figure 10**).

3.2.4. Utilization of the IMO Algorithm for Okumura-Hata Model Optimization

In this section, we will present the IMO algorithm can be applied in the optimization of the Okumura-Hata propagation model.

To optimize the Okumura-Hata model, the IMO algorithm will be considered as a black box that will take a vector K as input as defined by the factorized form of the K factor model and the data collected from the radio measurements. The methodological approach is presented by the following organizational chart.

In this chart of **Figure 11**; data filtering is made according to the criteria for distance and signal strength received (**Table 7**).

Radio measurements and the factorized form of the K-factor model are used to define the evaluation function.

Table 7. Filtering criteria.

Criterion	Distance (m)	Power (dBm)
Minimum	100	−110
Maximum	1000	−40

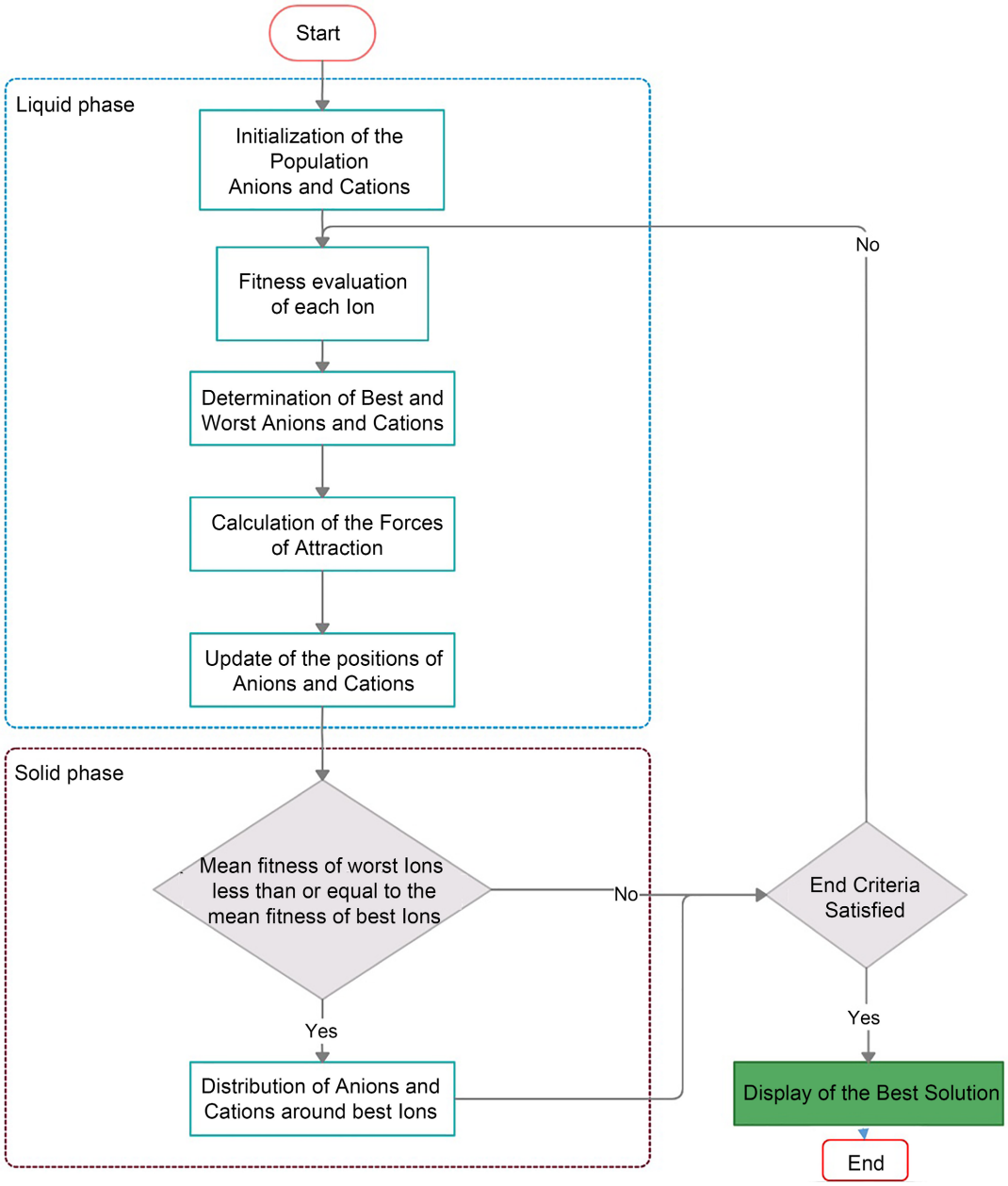

Figure 10. IMO algorithm execution flowchart [16].

The idea here is to show that using drive test data, the *k*-factors model equation and IMO algorithm, we can obtain a suitable propagation model for a given frequency and a specific environment. This is illustrated below in **Figure 12**.

3.3. Evaluation Function

The evaluation function accurately represents the input parameter of the IMO algorithm because it integrates the K factor model and radio measurement data. Using this evaluation function as an input parameter of the IMO algorithm aims to minimize the Euclidean distance between field measurements (real measurements) and those of predictions from the new model ($L = K \times M$).

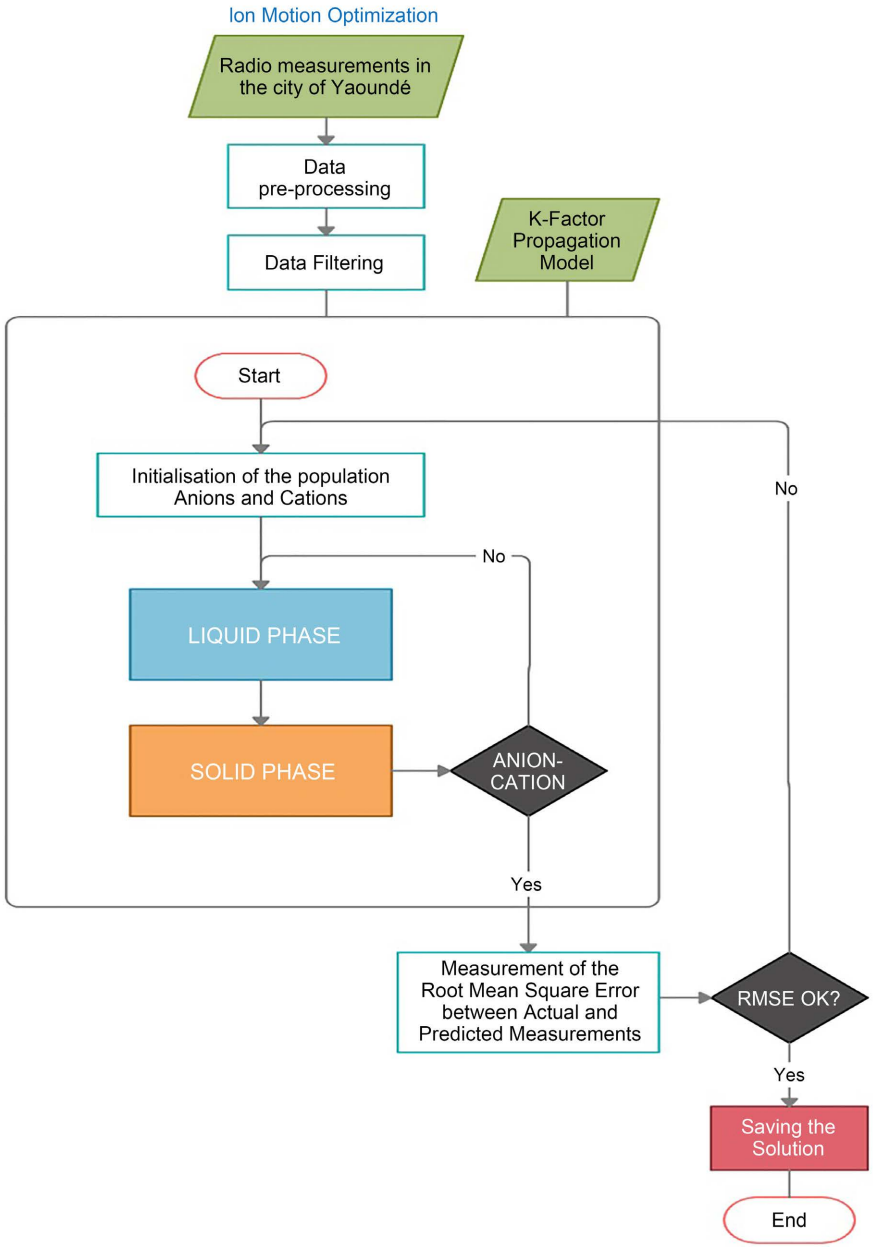

Figure 11. IMO optimization flow chart applied Okumura-Hata model.

Figure 12. IMO optimization method apply to propagation model optimization.

Let $L_M = \{L_i\}_{i=1:N}$ a vector representing the set of values of the losses measured for N points at N given distances. Note also that the vector M of equation

(10) depends on the distance d for d seen as a variable, that is a function of d; $M = f(d)$. Thus, for N measuring points at different distances d_i, M will become a matrix of 6 rows and N columns.

The objective function will therefore be:

$$f = \min\left\{\frac{1}{N}\sum_{i=1}^{N}\left(L_M(i)-(K\times M_i)\right)^2\right\} \tag{17}$$

The formula of the link balance between a measuring point and the BTS provides the received power presented as follows:

$$P_{\text{received}} = P_{\text{BTS}} + G_{\text{BTS}} + G_{\text{MS}} - \sum L_f - L_{\text{Measured}} \tag{18}$$

thus,

$$L_{\text{Measured}} = P_{\text{BTS}} + G_{\text{BTS}} + G_{\text{MS}} - \sum L_f - P_{\text{received}} \tag{19}$$

P_{received} represents the power received at each measuring point; P_{BTS} the transmission power of the BTS; G_{BTS} the gain of the BTS antenna; G_{MS} the gain of the mobile station; L_f losses induced by cables and connectors and L_{Measured} the value of measured losses. In addition, the values of the different distances are also implicit and are obtained from (the longitude and latitude of the BTS considered) and (the longitude and latitude of each measuring point). The method of determining the distance is as follows:

- **BTS-MS Distance Assessment**

Consider two points A and B of GPS coordinates presented as below (Table 8) and R the average radius of the earth in the area containing A and B, with R = 35,786 km at the equator.

The calculation of the Euclidean distance between A and B is given by the relation below:

$$D = R\times\arccos\left(\sin(a)\times\sin(b)-\cos(a)\times\cos(b)\times\cos(c-d)\right) \tag{20}$$

Considerations relating to the processing of data from radio measurements; the establishment of the evaluation function; to the generation of the basic family made within the framework of the city of Yaoundé are the same used in the city of Bertoua. However, given the fact that we are now working in 4G, the link budget will be different.

➢ **Link Budget for eLTE network**

The total power of an enodeB is evenly distributed across all available block resources.

The number of resources (RB) block $\text{Number}_{\text{RB}} = 5 \times B$ (only for B = 3, 5, 10, 15 and 20) With B the available spectrum width, If the total power of the eNodeB is P_{eNodeB} in W, the power per subcarrier will be:

Table 8. Notation used for longitude and latitude.

Points	A	B
Latitude	a	b
Longitude	c	d

$$P_{\text{sub-carrier}}(\text{W}) = \frac{P_{\text{enodeB}}}{N_{\text{sub-carrier}}}, \tag{21}$$

where $N_{\text{sub-carrier}}$ is the number of subcarriers

Then

$$P_{\text{sub-carrier}}(\text{dB}\cdot\text{m}) = P_{\text{enodeB}}(\text{dB}\cdot\text{m}) - 10\log_{10}(N_{\text{sub-carrier}}) \tag{22}$$

with

$$N_{\text{sub-carrier}} = \text{Number}_{\text{RB}} \times \text{Number}_{\text{sub-carrier per RB}} \tag{23}$$

Each RB consists of 12 LTE subcarriers. It is the power per subcarrier that will then be used in the link balance.

$$\begin{aligned} P_{\text{received}} = {} & P_{\text{sub-carrier}} + G_{\text{eNodeB}} + G_{\text{MS}} - \sum L_f - L_{\text{Measured}} - P_{\text{penetration}} \\ & - M_{\text{Interference}} - M_{\text{Fading}} \end{aligned} \tag{24}$$

Thus,

$$\begin{aligned} L_{\text{Measured}} = {} & P_{\text{sub-carrier}} + G_{\text{eNodeB}} + G_{\text{MS}} - \sum L_f - P_{\text{received}} - P_{\text{generation}} \\ & - M_{\text{Interference}} - M_{\text{Fading}} \end{aligned} \tag{25}$$

$P_{\text{penetration}}$ represents the penetration losses, $M_{\text{Interference}}$ represents the interference margin and M_{Fading} the fading margin. The power of the eNodeBs that was considered is 46 dBm and the frequency 400 Mhz.

At the end of the execution of the algorithm for each of the three districts of Bertoua we will have the vectors K_{Central}; K_{CRTV}; $K_{\text{Lycée}}$ each consisting of six parameters in the format $[K_1K_2K_3K_4K_5K_6]$ we will have a vector

$$K_{\text{Bertoua}} = [K_{1\text{Mean}}K_{2\text{Mean}}K_{3\text{Mean}}K_{4\text{Mean}}K_{5\text{Mean}}K_{6\text{Mean}}] \tag{26}$$

whose value of each of its parameters comes from the average of the parameters of the three cities considered above.

3.4. Generation of the Basic Family

The research space is between the standard Okumura-Hata model and the free space propagation model that characterizes barrier-free propagation.

The base family will be generated according to the algorithm below:

Algorithm

Begin

$K_{1el} = 32.4 + 20 \times log10(Fc);$

$K_{1ok} = 69.55 + 26.16 \times log10(Fc);$

For i = 1: Population Size

$K_1 = K_{1el} + (K_{1ok} - K_{1el}) \times rand(1);$

$K_3 = -2.49 + 2.49 \times rand(1)$

$K_4 = rand(1)$

$K_5 = -13.82 + 13.82 \times rand(1);$

$K_6 = -6.55 \times rand(1);$

$K_2 = 20 - (K_6 \times log10(H_b) + ((36.8 - 20) \times rand(1));$

$P(i,:) = [K_1K_2K_3K_4K_5K_6];$

End For

End

(27)

This pseudo-code is very important because it defines integrity constraints for each of the parameters K_1, K_2, K_3, K_4, K_5 and K_6. Fixing the order of magnitude of their respective values.

In this code, K_{1ok} represents the parameter K_1 in the Okumura-Hata model; K_{1el} represents the parameter K_1 for the free space model. P is the matrix representing the generated population and the population size corresponds to the number of distances measured.

3.5. IMO Algorithm Shutdown Criterion

The execution of the IMO algorithm is stopped only when it is certain that it has reached the overall optimum. That is to say, a global convergence in the research space.

This optimum is marked by obtaining the best ion in other words the ion for which its values of the six K parameters give the most minimal value to the objective function. At the optimum, the value of the anion is identical to that of the cation since they converged towards the same point.

Acceptance criterion for an optimized propagation model

An optimized propagation model is accurate if the square root of the mean quadratic error between actual and prediction measurements is less than 8 dB [19]-[25]. Therefore, after obtaining the best ion at the end of the execution of the IMO algorithm, we calculate the square root of the aptitude function for the values of K corresponding to this ion. This will involve calculating root mean square error which is the square root of the evaluation function as follows:

$$\text{RMSE} = \sqrt{\frac{1}{N}\sum_{i=1}^{N}\left(L_M(i)\right) - \left(K \times M(i)\right)^2} \tag{28}$$

The solution is saved only if RMSE < 8 dB which materializes at the end of the optimization process [19]-[25].

Table 9 presents the mathematic symbols used in the method part and their meaning.

4. Results

The following parameters (Figure 13) were used for IMO implementation, Number of cations and number of anions are set to 100, the maximum number of iterations is 100, Q_1 and Q_2 of conditions (16) are random numbers within the range [−1, 1] and rand( ) is a function that returns a random number within the

Table 9. Meaning of mathematic symbols used.

Symbol	Meaning	Symbol	Meaning
Σ	Sum of elements	**C**	cation
K	Vector representing an ion	**A**	anion
L_M	Measured Loss from DT	**RMSE**	Root mean square error
M	Specific vector defined by Equation (5)		

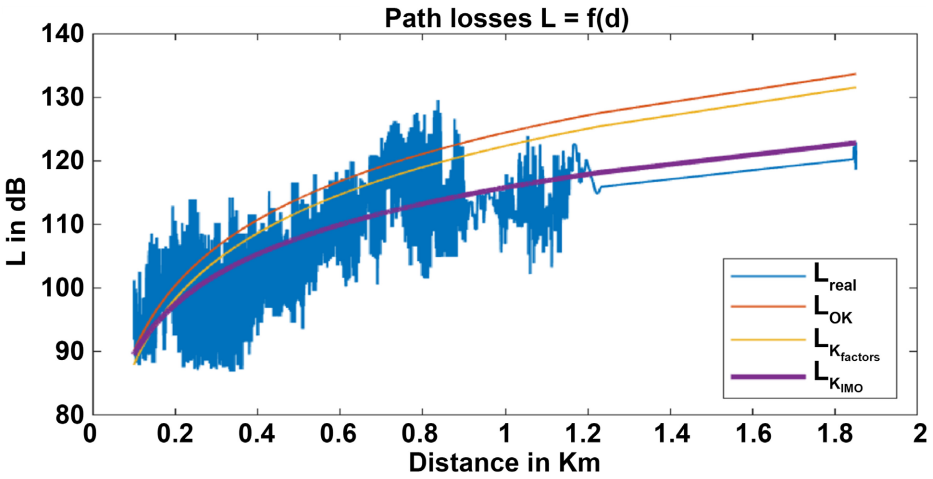

Figure 13. Actual measurements in the downtown VS predicted measurements.

interval [0, 1]. By area, we obtained the curves in Figure 13 representing the actual measurements in blue, the Okumura Hata model in pink, the standard K factors model in yellow, the model obtained by implementing the IMO algorithm in purple.

4.1. Results in Yaoundé

1) Dense urban area (A)

Center town Yaoundé (A1)

Table 10 shows a comparison of the value of the root mean square error for each of the models considered on the curve for the case of the downtown.

We note that we have an RMSE < 8 dB for the new model which confirms the reliability of the result, unlike the model *K* factor and Okumura Hata.

Bastos Yaounde (A2)

Bastos district (A2 embassy districts) (Figure 14)

Table 11 shows a comparison of the value of the root mean square error for each of the models considered on the curve for the case of the Bastos district.

We note that we have an RMSE < 8 dB which confirms the reliability of the result.

2) Urban area (B)

- Biyem-Assi district (B1) (Figure 15)

Table 12 presents a comparison of the value of the mean square error for each of the models considered on the curve for the case of the Biyem-Assi district.

We note that we have an RMSE < 8 dB which confirms the reliability of the result.

Mvog-Ada (B2)

Table 13 shows a comparison of the value of the root mean square error for each of the models considered on the curve for the case of the Essos district.

- We note that we have a RMSE < 8 dB which confirms the reliability of the result (Figure 16).

Table 10. Results in downtown.

Zone	Results	K_1	K_2	K_3	K_4	K_5	K_6	RMSE
	IMO	132.1130	33.6958	−1.3151	0.5817	−9.0232	−4.6322	6.4256
A1	Okumura hata	146.56	44.9	0	0	−13.82	−6.55	14.9345
	K factors	149	44.9	−2.49	0	−13.82	−6.55	13.8041

Table 11. Results in Bastos.

Zone	Results	K_1	K_2	K_3	K_4	K_5	K_6	RMSE
	IMO	135.4566	22.7274	−1.4100	0.6188	−8.7619	−1.8613	6.5346
A2	Okumura hata	146.56	44.9	0	0	−13.82	−6.55	11.2924
	K factors	149	44.9	−2.49	0	−13.82	−6.55	10.5121

Table 12. Results in biyem Assi.

Zone	Results	K_1	K_2	K_3	K_4	K_5	K_6	**RMSE**
	IMO	128.0936	28.6472	−1.1890	0.6492	−6.9251	−5.2888	**5.8527**
B1	Okumura hata	146.56	44.9	0	0	−13.82	−6.55	**12.3604**
	K factors	149	44.9	−2.49	0	−13.82	−6.55	**11.3767**

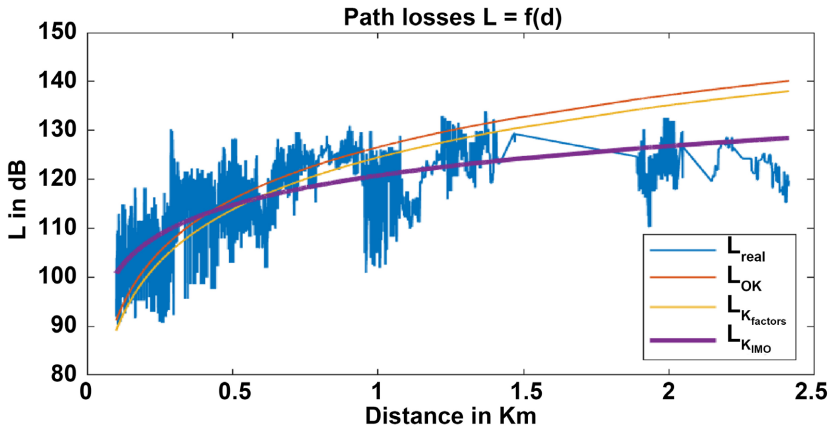

Figure 14. Actual measurements Bastos VS predicted measures.

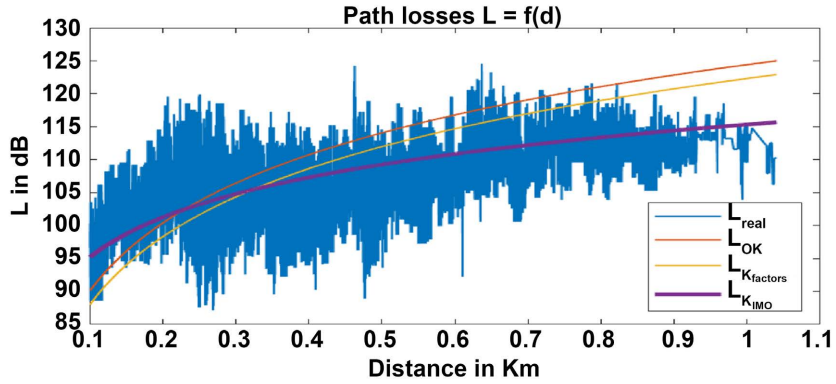

Figure 15. Actual measurements Biyem Assi VS Predicted Measurements.

Table 13. Results in Essos.

Zone	Results	K_1	K_2	K_3	K_4	K_5	K_6	**RMSE**
	IMO	133.6745	30.3813	−1.4091	0.7667	−6.8991	−3.2156	**7.2967**
B2	Okumura hata	146.56	44.9	0	0	−13.82	−6.55	**11.5989**
	K factors	149	44.9	−2.49	0	−13.82	−6.55	**10.6673**

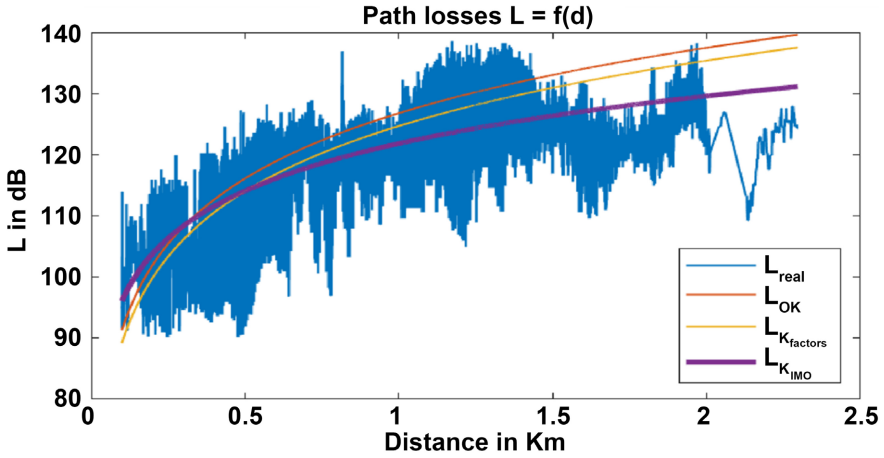

Figure 16. Actual measurements Mvog Ada VS predicted measures.

Table 14 shows a comparison of the value of the root mean square error for each of the models considered on the curve for the case of the Essos district.

3) Suburban Area (C)

- Nkomo Awae (C1)

Table 14 presents a comparison of the value of the root mean square error for each of the models considered on the curve for the case of the Nkomo district.

We note that we have a RMSE > 8 dB, this is explained by the complex morphology of the Nkomo Awae district (Figure 17), however the solution obtained is of better quality than the models of Okumura Hata and K factors.

- Ngousso Eleveur district (C2) (Figure 18)

Table 15 presents a comparison of the value of the root mean square error for each of the models considered on the curve for the case of the Ngousso district.

We note that we have a RMSE < 8 dB which confirms the reliability of the result.

Given these different results, we note that the IMO algorithm has considerably minimized the value of the RMSE in each of the districts of the city of Yaoundé. Although in the Nkomo district its value is slightly above the maximum value of the RMSE, a margin was tolerated and all these cities were taken into account in the estimation of the average *K* vector to obtain the global propagation model of the city of Yaoundé presented in Figure 21 above.

The final expression of our model of propagation of the city of Yaoundé is therefore:

Table 14. Results in Nkomo Awae.

Zone	Results	K_1	K_2	K_3	K_4	K_5	K_6	RMSE
	IMO	131.0273	42.5740	−0.9474	0.6793	−3.5878	−4.2929	9.0405
C1	Okumura hata	146.56	44.9	0	0	−13.82	−6.55	15.3274
	K factors	149	44.9	−2.49	0	−13.82	−6.55	14.4380

Table 15. Results in Ngousso Eleveur.

Zone	Results	K_1	K_2	K_3	K_4	K_5	K_6	RMSE
	IMO	132.7396	29.6835	−0.9693	0.4461	−8.4451	−2.6861	8.0198
C2	Okumura hata	146.56	44.9	0	0	−13.82	−6.55	16.8067
	K factors	149	44.9	−2.49	0	−13.82	−6.55	15.7616

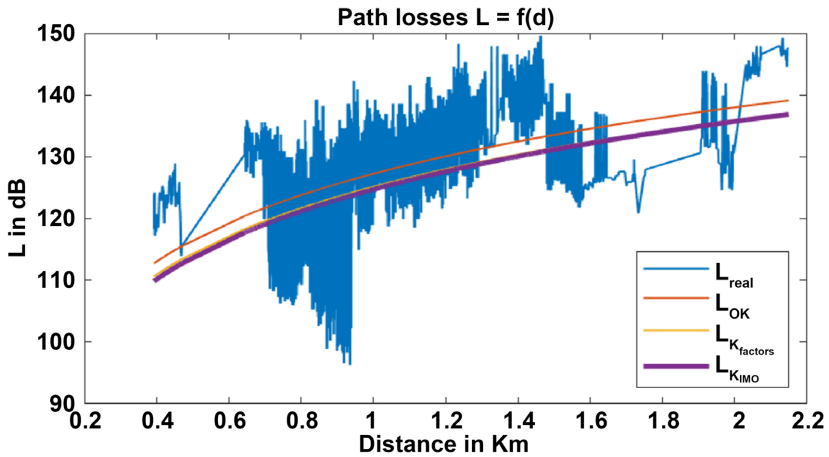

Figure 17. Actual measurements Nkomo Awae VS predicted measures.

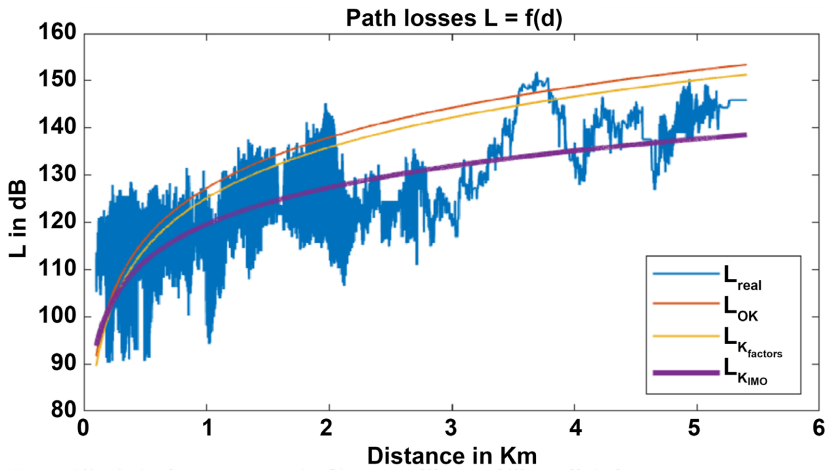

Figure 18. Actual measurements Ngousso Eleveur VS predicted measures.

$$L = 132.1841 + 31.2849 \times \log(d) + (-1.2067) \times H_m + 0.62367 \times \log(H_m) + (-7.2737) \times \log(H_b) + (-3.6628) \times \log(H_b) \times \log(d) \quad (29)$$

The results obtained in the city of Yaoundé allowed us to validate the performance of the IMO algorithm about the resolution of complex problems including the optimization of propagation models. The results obtained in the city of Bertoua through a drive test done in an LTE TDD network with a spectrum between 380 MHz to 400 MHz are presented in the following.

4.2. Results in Bertoua

Propagation attenuation graphs as a function of distance.

In each of the areas considered in the city center of the city of Bertoua we obtained the following graphs:

- Bertoua Central

In this Figure 19, the model optimized with IMO is much more similar to the actual measurements of the Bertoua Central area compared to the Okumura-Hata and K Factors models.

- Bertoua CRTV

In this scheme of Figure 20, the model optimized with IMO is much more similar to the actual measurements of the Bertoua CRTV area compared to the Okumura-Hata and K Factors models.

- Bertoua Lycee

In this Figure 21, the model optimized with IMO is much more similar to the actual measurements of the Bertoua Lycée area compared to the Okumura-Hata and *K* Factors models.

➢ **Interpretation**

The RMSE values for each of the zones are recorded in Table 16:

Table 16. RMSE values.

Area	K_1	K_2	K_3	K_4	K_5	K_6	RMSE
Bertoua Central	106.0086	32.3922	−1.5946	0.4493	−0.6007	−4.4267	6.7313
Bertoua CRTV	110.8726	37.3906	−0.6667	0.4431	−6.0063	−4.9540	6.2458
Bertoua lycée	115.4539	34.7907	−1.8135	0.6213	−7.3535	−3.3966	7.1411

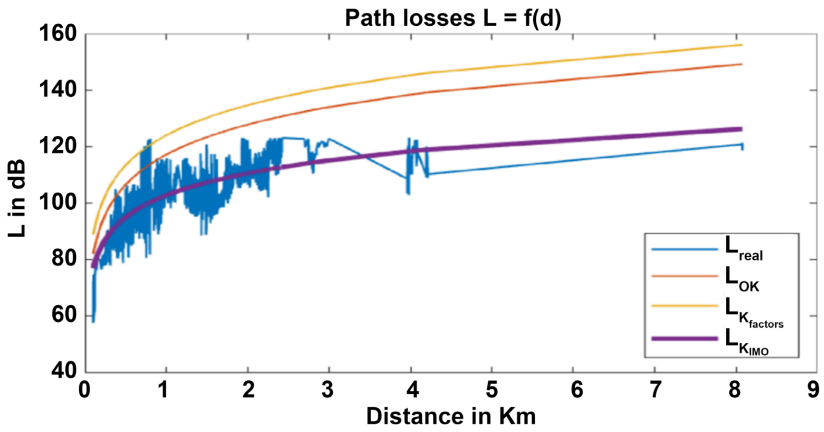

Figure 19. Actual measurements Bertoua Central VS predicted measures.

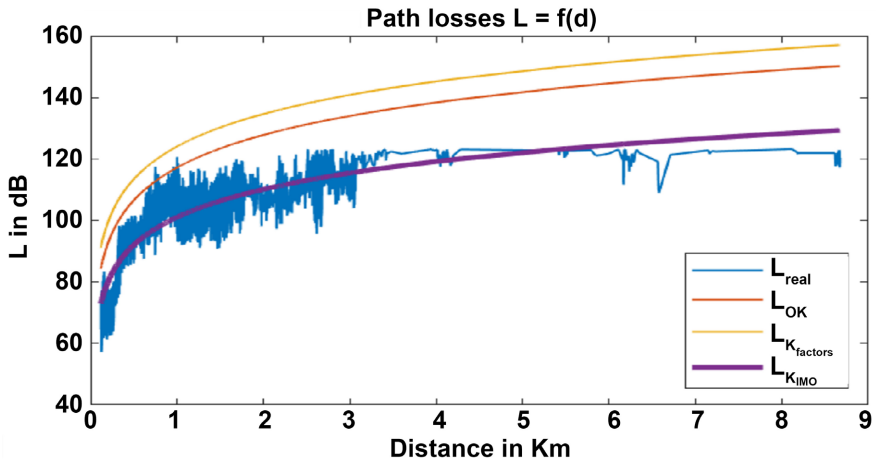

Figure 20. Actual Bertoua CRTV vs predicted measurements.

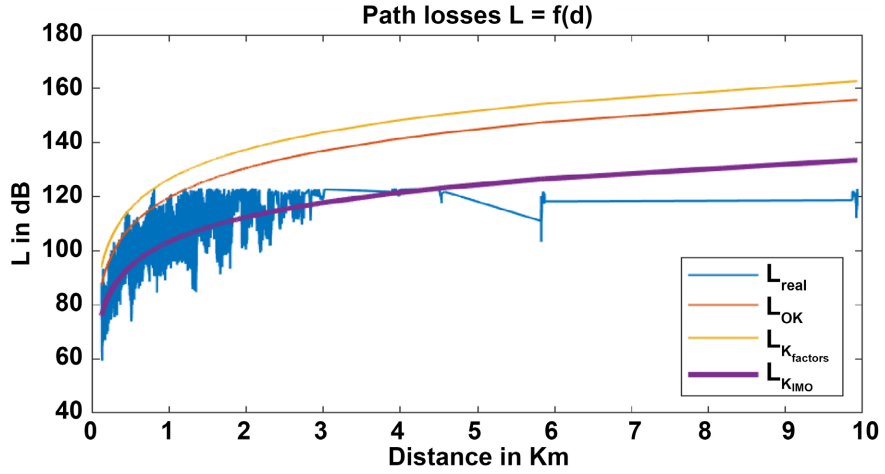

Figure 21. Actual Bertoua Lycée vs predicted measurements.

Optimization is generally good in each of the areas considered. The RMSE value < 8 dB in each of them proves the reliability of the result. Thus, all three zones are taken into account in the development of the final propagation model.

4.3. Summary of Results

In all the three areas above; the RMSE obtained through the new model made up using IMO is better than the one calculated using Okumura Hata Model. The optimal propagation model retained for Bertoua is presented in Table 17.

The final expression of the propagation model that we propose for the city of Bertoua is therefore:

$$L = 110.7783 + 34.8578 \times \log(d) + (-1.3583) \times H_m + 0.50459 \times \log(H_m) + (-4.6535) \times \log(H_b) + (-4.2591) \times \log(H_b) \times \log(d) \quad (30)$$

The optimized propagation models for the 02 cases of this study can be used for the deployment of any technology including 5G and LPWAN technologies like LoRAWAN, SIGFOX, NB-IoT and LTE-M which are suitable for IoT network

Table 17. Final K values.

Method	K_1	K_2	K_3	K_4	K_5	K_6
Solution	**110.7783**	**34.8578**	**−1.3583**	**0.50459**	**−4.6535**	**−4.2591**

if there are deployed in 800 MHz or in 400 MHz. The propagation model in fact is not link to the technologies, Okumura Hata and Cost 231 models developed longtime before for Television broadcasting and GSM network are still used to build 3G, 4G and 5G network with respect to the frequency range for which the models have been developed, in the same way, the ones proposed in this study can be used. Another advantage is that, we proposed a method which can be used to optimize propagation model in any kind of town once the drive tests data and radio parameters are available, globally the proposed method can help for improving newly the development of new networks like the one of IoT (LoRaWAN, SIGFOX, NB-IoT and LTE).

5. Conclusion

In this paper we have used the IMO algorithm to aim to solve the problem of propagation model optimization. We have considered for that 02 towns in Cameroon, Yaoundé town where a drive test has been done on a CDMA 2000 network and the town of Bertoua where data were collected on an LTE TDD network. After implementing IMO use modeling based on a modified K factor model we obtained a propagation model of the Yaoundé city with RMSE value between 5.8527 dB and 9.0405 dB while that of the Okumura-Hata model varies from 11.29 dB to 16.80 dB and that of the K model factor of 10.51 dB and 15.76 dB. Based on these results, the performance of the IMO algorithm for the optimization of propagation models has been proven. Thus, the same work was carried out in the city of Bertoua as part of the smart cities deployment project whose results provided RMSE values ranging from 6.2458 to 7.1411. We deduce that the new models are more accurate and better represent the wireless propagation in each of the two cities of Yaoundé and Bertoua. We can conclude that the IMO algorithm can perform well in solving this kind of problem.

Conflicts of Interest

The authors declare no conflicts of interest regarding the publication of this paper.

References

[1] Beasley, D., Bull, D. and Martin, R. (1993) An Overview of Genetic Algorithms. Part 2. University of Cardiff, Cardiff.

[2] Beasley, D., Bull, D. and Martin, R. (1993) An Overview of Genetic Algorithms. Part 1. University Cardiff, Cardiff.

[3] Fogel, D.B. (2000) What Is Evolutionary Computation. *IEEE Spectrum*, **37**, 26-32. https://doi.org/10.1109/6.819926

[4] Goldberg, D.E. (1989) Genetic Algorithms in Search, Optimization and Machine Learning. Addison Wesley, Reading.

[5] Mitchell, M. (1996) An Introduction to Genetic Algorithms. MIT Press, Cambridge.

[6] Kennedy, J. and Eberhart, R.C. (1997) A Discrete Binary Version of the Particle Swarm Algorithm. 1997 *IEEE International Conference on Systems, Man, and Cybernetics. Computational Cybernetics and Simulation*, Orlando, 12-15 October 1997, 4104-4108.

[7] Kennedy, J. and Eberhart, R.C. (1995) Particle Swarm Optimization. *Proceedings of IEEE International Conference on Neural Networks*, Perth, 27 November-1 December 1995, 1942-1948.

[8] Clerc, M. and Kennedy, J. (2002) The Particle Swarm: Explosion, Stability and Convergence in Multi-Dimensional Complex Space. *IEEE Transactions on Evolutionary Computation*, **20**, 1671-1676.

[9] Nezami, O.M., Bahrampour, A. and Jamshidlou, P. (2013) Dynamic Diversity Enhancement in Particle Swarm Optimization (DDEPSO) Algorithm for Preventing from Premature Convergence. *Procedia Computer Science*, **24**, 54-65. https://doi.org/10.1016/j.procs.2013.10.027

[10] Akay, B. and Karaboga, D. (2012) A Modified Artificial Bee Colony Algorithm for Real Parameter Optimization. *Information Sciences*, **192**, 120-142. https://doi.org/10.1016/j.ins.2010.07.015

[11] Karaboga, D. and Akay, B. (2009) A Comparative Study of Artificial Bee Colony Algorithm. *Applied Mathematics and Computation*, **214**, 108-132. https://doi.org/10.1016/j.amc.2009.03.090

[12] Karaboga, D. and Basturk, B. (2008) On the Performance of Artificial Bee Colony (ABC) Algorithm. *Applied Soft Computing*, **8**, 687-697. https://doi.org/10.1016/j.asoc.2007.05.007

[13] Karaboga, D. (2005) An Idea Based on Honey Bee Swarm for Numerical Optimization. Technical Report-TR06.

[14] Gu, W., Yin, M. and Wang, C. (2012) Self Adaptive Artificial Bee Colony for Global Numerical Optimization. *IERI Procedia*, **1**, 59-65. https://doi.org/10.1016/j.ieri.2012.06.011

[15] Javidya, B., Hatamloua, A. and Mirjalili, S. (2015) Ions Motion Algorithm for Solving Optimization Problems. *Applied Soft Computing*, **32**, 72-79. https://doi.org/10.1016/j.asoc.2015.03.035

[16] Nguyen, T.-T., Wang, M.-J., Pan, J.-S., Dao, T.-K. and Ngo, T.-G. (2020) A Load Economic Dispatch Based on Ion Motion Optimization Algorithm. In: Pan, J.S., Li, J., Tsai, P.W. and Jain, L., eds., *Advances in Intelligent Information Hiding and Multimedia Signal Processing*, Springer, Singapore. https://doi.org/10.1007/978-981-13-9710-3_12

[17] Nguyen, T.T. and Dao, T.T. (2019) Applications of Ion Motion Optimization Algorithm in the Travelling Salesman Problem. *IOSR Journal of Computer Engineering*, **21**, 60-65.

[18] Trong-The, N., Jeng-Shyang, P. and Tsu-Yang, W. (2019) Node Coverage Optimization Strategy Based on Ions Motion Optimization. *Journal of Network Intelligence*, **4**, 1-9.

[19] Deussom, E. and Tonye, E. (2015) New Propagation Model Optimization Approach Based on Particles Swarm Optimization Algorithm. *International Journal of Computer Applications*, **11**, 39-47. https://doi.org/10.5120/20785-3430

[20] Deussom, E., Tonye, E. and Kabiena, B. (2020) Propagation Model Optimization Based on Artificial Bee Colony Algorithm: Application to Yaoundé Town, Cameroon. *IOSR Journal of Electrical and Electronics Engineering* (*IOSR-JEEE*), **15**, 14-26.

[21] Deussom, E., Souop, K.G.D.D., Feudjio, C., Tonye, E. and Michael, E.S. (2022) Social Spider Algorithm-Based Approach for Propagation Model Optimization. Application to Yaounde Town. *International Journal of Engineering Research & Technology*, **11**, 527-533.

[22] Tonye, E. and Deussom, E. (2015) Optimisation de modèles de propagation à partir des données de mesures radio de la ville de Yaoundé. *Journal of the Cameroon Academy of Sciences*, **12**, 180-205.

[23] Deussom, E. and Tonye, E. (2015) New Approach for Determination of Propagation Model Adapted to an Environment Based on Genetic Algorithms: Application to the City of Yaoundé, Cameroon. *IOSR Journal of Electrical and Electronics Engineering*, **10**, 48-59.

[24] Deussom, E. and Tonye, E. (2015) Optimization of Okumura Hata Model in 800 MHz Based on Newton Second Order Algorithm. Case of Yaoundé, Cameroon. *IOSR Journal of Electrical and Electronics Engineering* (*IOSR-JEEE*), **10**, 16-24.

[25] Deussom, E. and Tonye, E. (2015) Optimisation du modèle d'Okumura Hata par la régression linéaire. Application à la ville de Yaoundé au Cameroun. *IOSR Journal of Electronics and Communication Engineering* (*IOSR-JECE*), **10**, 63-72.